

Elastic *vs.* inertial instability in a polymer solution flow

A. GROISMAN and V. STEINBERG

*Department of Physics of Complex Systems, The Weizmann Institute of Science
76100 Rehovot, Israel*

(received 24 November 1997; accepted in final form 29 May 1998)

PACS. 47.20-k – Hydrodynamic stability.

PACS. 83.50Eb – Weissenberg effect.

Abstract. – The interrelation between elastic and inertial effects in destabilizing the flow of a polymer solution is studied experimentally. To achieve this goal, solution elasticity is varied by three orders of magnitude and a diagram of the flow states in a Couette-Taylor system is obtained. The regions of purely elastic and purely inertial flow instabilities and a crossover region between them are characterized. The main feature of the elastic instability, constant Deborah number at the instability threshold, is verified. An analogy between inertial and elastic flow transitions and dynamics is found and the concept of *viscoelastic similarity* is introduced.

Elastic phenomena in flows of polymer solutions have lately been attracting increasing attention of physicists [1]. One of the reasons for this growth of interest is the discovery of “purely elastic” flow instabilities [2-4]. It has been found that elastic stresses that depend on flow velocity in a non-linear way can destabilize a polymer solution flow. So, dramatic flow transitions can occur even at vanishingly small Reynolds number, Re , when inertial effects are negligible. The investigation of the purely elastic instabilities and patterns above the instability threshold is interesting not only because it opens a new class of pattern forming systems. In the absence of inertial forces, it also presents the simplest situation, where non-linear elastic behavior of polymeric liquids in complex three-dimensional flows can be studied. Understanding of general laws of this behavior is an issue of major importance for approaching the problem of turbulent drag reduction by polymer additives [5]. It is one of the long-standing problems in fluid mechanics that is hard to attack directly, since inertial and elastic non-linearities are both essential there.

The purpose of the experiments reported in this letter was to explore the general similarity features in a polymer solution flow in the purely elastic regime, and to find out how the ratio of elastic-to-inertial effects depends on the properties of the polymer solution. In order to do that, flow transitions in a Couette-Taylor (CT) system were studied. A CT system is a simple arrangement of two coaxial cylinders with a working fluid in the annular gap between them. If the fluid is Newtonian and the rotation velocity, Ω , of the inner cylinder is gradually increased, at some critical Reynolds number, Re_c , the basic purely azimuthal Couette flow becomes unstable. (The outer cylinder is stationary in our system.) As a result

of the instability, a stationary axisymmetric pattern of the Taylor vortex flow (TVF) arises [6]. This Taylor instability is driven by centrifugal force, so it is inertial in its nature.

The behavior of viscoelastic polymer solutions in the CT geometry can be quite different from that of usual Newtonian fluids. This is mainly because of negative normal stress difference, $N_1 = \tau_{\theta\theta} - \tau_{rr}$ (r , θ and z are cylindrical coordinates), that is generated in polymer solutions in Couette flow [5,3]. The stress difference grows with the shear rate, $\dot{\gamma}_{r\theta}$, and since the CT geometry is curvilinear, it produces a volume force, N_1/r , acting inwards in the radial direction that is sometimes called ‘‘hoop stress’’. In highly elastic polymer solutions this hoop stress can be much stronger than the centrifugal force, and then the well-known phenomenon of ‘‘rod-climbing’’ (Weissenberg effect) [5] is observed. It is natural to suppose that a large hoop stress can make the Couette flow unstable. Such instability would be purely elastic in the sense that the fluid inertia would be of no importance there.

Observation of a purely elastic instability in CT flow was first reported by Larson, Muller and Shaqfeh [2], who also proposed a criterion of instability driven by the hoop stress [7]. The calculations in [7] were based on the Oldroyd-B model [5,3], which is a reasonably good description of dilute solutions of polymers in viscous Newtonian solvents (Boger fluids [8]) used by the authors. In the Oldroyd-B model, the stress tensor is given by $\boldsymbol{\tau} = \boldsymbol{\tau}^s + \boldsymbol{\tau}^p$. The contribution $\boldsymbol{\tau}^s = -\eta_s \dot{\boldsymbol{\gamma}}$, where $\dot{\boldsymbol{\gamma}}$ is the rate-of-strain tensor, is due to Newtonian viscosity of the solvent, η_s . The polymer part of the stress is given by $\boldsymbol{\tau}^p + \lambda \boldsymbol{\tau}_{(1)}^p = -\eta_p \dot{\boldsymbol{\gamma}}$, where λ is the polymer relaxation time and $\boldsymbol{\tau}_{(1)}^p$ is a convected time derivative of $\boldsymbol{\tau}^p$ [5,3]. In stationary plane shear flow, $v_x = \dot{\gamma}_{xy}y$, the polymer shear stress is $\tau_{xy}^p = -\eta_p \dot{\gamma}_{xy}$. Thus, an apparent solution viscosity, $\eta = \eta_p + \eta_s$, can be introduced such that $\tau_{xy} = -\eta \dot{\gamma}_{xy}$.

The normal stress difference in CT flow, which is a non-linear effect, is given by the Oldroyd-B model as $N_1 = \tau_{\theta\theta} - \tau_{rr} = -2\eta_p \lambda (\dot{\gamma}_{r\theta})^2$. In a CT system with a small gap size, $d \ll R_1$, where R_1 is the inner cylinder radius, the shear rate $\dot{\gamma}_{r\theta}$ is almost constant across the gap and equal to $\Omega R_1/d$. The product $\lambda \dot{\gamma}_{r\theta}$ is called the Deborah number, De. Since $\text{De} = N_1/(2\tau_{r\theta}^p)$, it defines the ratio between non-linear and dissipative terms in the Oldroyd-B model that is quite analogous to the role of Reynolds number in the Navier-Stokes equation. At fixed gap ratio, d/R_1 , and polymer contribution to viscosity, η_p/η , the elastic instability is predicted to occur when De is raised above a certain threshold which is independent of λ [7].

A parameter that reflects the relative importance of elastic and inertial effects is the ratio between the Deborah number and the Reynolds number, $\kappa = \text{De}/\text{Re}$, where $\text{Re} = \Omega R_1 d \rho / \eta$ and ρ is the fluid density. This parameter has another straightforward interpretation. It is the ratio, $\kappa = \lambda/t_{\text{vd}}$, between λ and the viscous diffusion time, $t_{\text{vd}} = d^2 \rho / \eta$.

In this letter we report the following main results. I) We have varied the solution elasticity, κ , by three orders of magnitude and have obtained a diagram of flow states in a very broad range of κ and De. It is shown how flow instability gradually changes its nature from the usual inertial to purely elastic as the elasticity is increased. II) For the first time, it is experimentally confirmed that at high elasticity, flow transitions occur at constant Deborah number. III) Investigation of the flow transitions in the purely elastic regime allowed us to introduce a concept of *viscoelastic similarity*.

In dilute polymer solutions, λ and η_p are both proportional to η_s so that $\kappa \sim \eta_s^2$. Therefore, by varying η_s we can investigate both the dependence of the flow stability on λ in the purely elastic regime and explore regions of different κ , with various ratios of the fluid elasticity to inertia. We realized this idea experimentally by using Newtonian solvents of different viscosity and by changing the temperature in the CT column. Two solutions of the same polymer (polyacrylamide, PAAm, $M_w = (5-6) \times 10^6$ [9]) with a concentration of 300 ppm were prepared. The Newtonian solvents were 63% and 53% saccharose in water for the first and the second polymer solution, respectively.

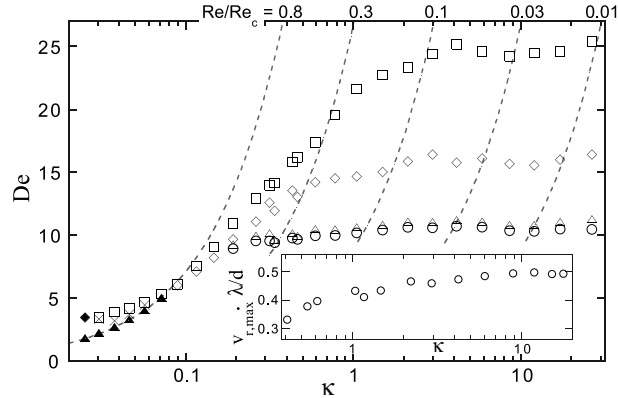


Fig. 1. – A diagram of states in the CT flow at various κ and De . Transitions between the flow states are denoted by different symbols. Squares: Couette flow (or RSW at $\kappa < 0.08$)-DO; open diamonds: DO-oscillatory strips (or Couette flow at $\kappa < 0.2$); open triangles: oscillatory strips-diwhirls; circles: diwhirls-Couette flow; solid triangles: Couette flow-TVF; crosses: TVF-RSW; solid diamond: TVF-Wavy mode. The dashed curves show the lines of constant Re corresponding to different values of Re/Re_c . Inset: $v_{r,\max}$ in diwhirls at their decay point multiplied by λ/d , as a function of κ .

Viscosities and relaxation times of the solutions were measured with the aid of HAAKE 100 viscometric system [9]. The experiments on CT flow were conducted in a temperature-controlled CT column with $R_1 = 34$ mm, $d = 7$ mm, and length $L = 516$ mm. The temperature was varied in steps of 2.5 °C from 37.5 to 5 °C for the first solution and from 40 to 10 °C for the second solution. In the explored temperature regions the ratio η_p/η was constant up to a few percent at 0.45 for both solutions, while η_s changed from 0.35 to 2.9 P and from 0.097 to 0.38 P for the first and the second solution, respectively. The polymer relaxation time λ approximately followed the relation $\lambda \sim \eta_s/T^2$, where T is the absolute temperature. In the studied temperature regions λ changed from 0.28 to 3.1 s for the first solution and from 0.085 to 0.41 s for the second solution, the overall variation of κ being from 0.025 to 27 . The CT flow was visualized by adding to the working fluid a small amount of light reflecting flakes (0.6% of Kalliroscope liquid). For local velocity measurements, the laser Doppler velocimetry (LDV) technique was used.

The diagram of states of the CT flow is presented in fig. 1 in coordinates κ and De . (One can see a good match between the flow states of the two solutions in the region of overlapping, $\kappa = 0.3$ – 0.5 .) When the elasticity, κ , is large, Re becomes completely irrelevant and all flow transitions occur at constant De . This is in complete agreement with the above theoretical prediction for the purely elastic instability. The sequence of flow states in the CT system at large κ is illustrated by the space-time diagram in fig. 2. If Ω is increased above a certain threshold, the basic Couette flow becomes unstable and a pattern of strong chaotic oscillatory vortex motion, that we call disordered oscillations (DO) [9,10], develops in the system. When κ is high, the critical Deborah number, De_c , at this transition asymptotically approaches $De_c^\infty \approx 25$. If De is abruptly raised from zero to a few percent above De_c (fig. 2), the transition from the Couette flow to DO occurs almost simultaneously over the whole CT column, and an ordered pattern of transient neutral linear oscillations, NLO [9], is observed. The transition to DO is strongly hysteretic [10], in good agreement with the recent theoretical prediction for the purely elastic instability [11]. When De is subsequently lowered, the flow patterns that appear include oscillatory strips (see fig. 2 after decreasing De to $0.55 De_c$) and stationary

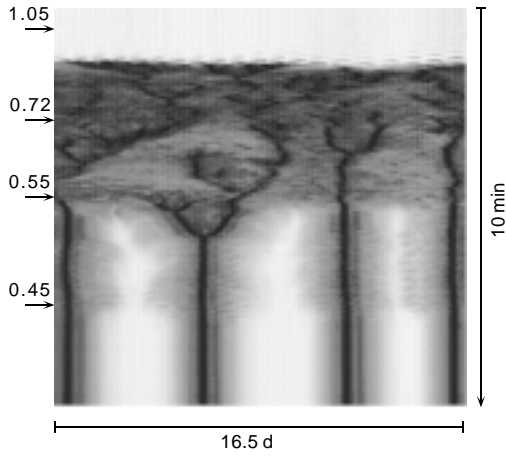


Fig. 2

Fig. 2. – A space-time diagram of different flow states and transitions between them at large κ . Ω was abruptly changed at the times shown by the arrows into the values written above them. $\Omega = 1$ corresponds to $De = De_c$.

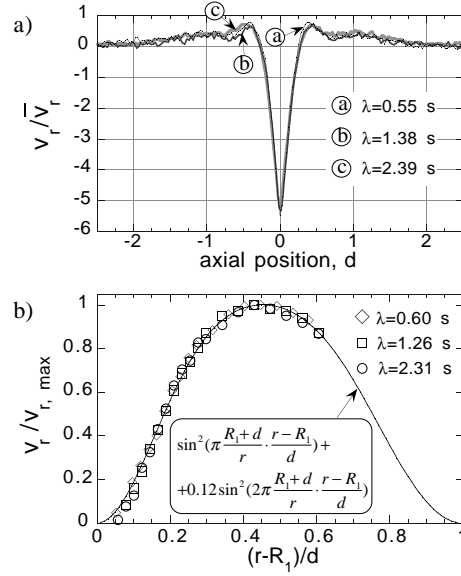


Fig. 3

Fig. 3. – a) Relative radial velocity, v_r/\bar{v}_r , in the diwhirls as a function of axial position at three different λ . v_r was measured at constant r near the middle of the gap, where it is maximal. b) Dependence of $v_r/v_{r,\max}$ in the middle of a diwhirl on the relative distance from the inner cylinder, $(r - R_1)/d$, at three different λ .

vortex structures (at $De = 0.45 De_c$) that we call solitary vortex pairs, or “diwhirls” [10]. The diwhirls decay, and the Couette flow is restored at $De \approx 10.5 \approx 0.42 De_c$.

When κ becomes smaller than about 2.5, De_c begins to decrease and the region of hysteresis between the onset of DO and the decay of the diwhirls begins to shrink. This occurs because the destabilizing inertial effects are no longer negligible ($Re/Re_c > 0.1$ at the DO onset). At $\kappa \simeq 0.15$ the oscillatory strips and the diwhirls cease to appear at all, and the DO decay directly to the Couette flow. At $\kappa \simeq 0.08$ inertial effects begin to dominate and, as for usual Newtonian fluids, stationary TVF appears as a result of instability of the Couette flow. This occurs at $De \approx 0.2 De_c^\infty$ and $Re \approx 0.8 Re_c$. The vicinity of this co-dimension-two point was described in more detail previously [9]. At larger De (and Re), TVF becomes unstable and gives way to a pattern of standing waves with $m = 1$ (rotating standing waves, RSW [9]). At even higher De , these RSW are changed by DO. At the leftmost point in fig. 1, at $\kappa = 0.025$, RSW and DO cease to appear. TVF gives way to the wavy mode [6] (at $De/De_c^\infty \approx 0.14$ and $Re/Re_c \approx 1.5$) characteristic for the inertial instability, so that the elastic effects are hardly noticeable. The transition from the Couette flow to TVF occurs at constant Re , almost independently of κ , so that TVF always remains an inertial mode. The reduction from Re_c to $0.8 Re_c$ can be partially due to shear thinning of the solution viscosity (the shear thinning of η was about 10% at the TVF threshold).

Just as TVF is a characteristic mode of the inertial instability, the diwhirls seem to be characteristic of the elastic instability. Indeed, the diwhirls decay at almost constant De over

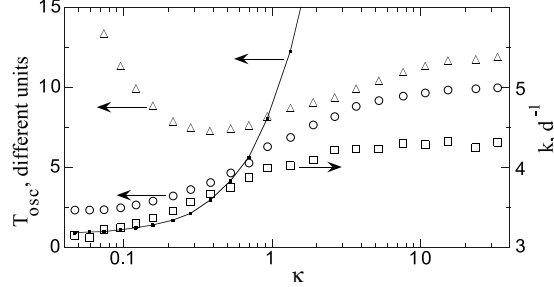


Fig. 4. – Oscillation period, T_{osc} , and the axial wave number (squares) of NLO, at $\text{De} = 1.03 \text{ De}_c$, as functions of elasticity, κ . T_{osc} is measured in units of λ (triangles), t_{vd} (points and continuous line) and $T_{\text{rot}} = 2\pi/\Omega$ (circles).

the whole region of their appearance, $\lambda = 0.30\text{--}3.1$ s, while Re at the decay point varies from 0.004 Re_c to 0.5 Re_c . As was previously shown [10], a diwhirl is a pair of vortices with intense inflow concentrated in a narrow region in the middle (dark lines in fig. 2) and slow outflow at the edges. The velocity profiles of the diwhirls turned out to be quite universal. This can be discerned from fig. 3a) where distributions of v_r along the z -axis at three different values of λ were plotted on the same axes by dividing by the root mean squares of the distributions, \bar{v}_r . Figure 3b) shows the dependence of v_r on r in the middle of a diwhirl, also at three different λ , that were plotted on the same axes by dividing by the maximal radial velocity, $v_{r,\text{max}}$. The dependence of $v_{r,\text{max}}$ on κ measured at De just above the diwhirl decay, is shown in the inset in fig. 1. One can see that at large κ the dimensionless variable $v_{r,\text{max}}\lambda/d$ asymptotically approaches a constant value of about 0.5.

The above observations allow us to draw an analogy between the inertial Taylor instability leading to TVF and the elastic instability resulting in the diwhirls. If the flow geometry is preserved so that $d/R_1 = \text{const}$, the threshold of the Taylor instability is determined by the Reynolds number, $\text{Re} = \Omega R_1 d \rho / \eta = t_{\text{vd}} \dot{\gamma}_{r\theta}$. Above the instability threshold, the TVF velocity profile depends only on Re/Re_c , and the characteristic velocity, v_r , of TVF at constant Re is proportional to d/t_{vd} . Both these results are due to hydrodynamic similarity that follows from the Navier-Stokes equation. The properties of the diwhirls become very similar to those of TVF, if we change t_{vd} into λ . Indeed, when d/R_1 and η_p/η are fixed, the diwhirls decay at constant $\text{De} = \lambda \dot{\gamma}_{r\theta}$ and the characteristic v_r at the diwhirl decay (at constant De) is proportional to d/λ . We note here that d/v_r defines the time of motion of a fluid element in the secondary flow (and, so, a time of variation of stress along the fluid trajectory), and v_r/d is the characteristic rate of strain in it. Thus, λ sets a universal time scale for the diwhirls just as t_{vd} sets it for TVF. Therefore, for the elastic instability we can speak about viscoelastic similarity, where De and λ play the same roles as Re and t_{vd} play in the usual hydrodynamic similarity.

In contrast to the diwhirls, the part of elastic and inertial forces in driving DO can vary quite significantly. Indeed, at $\kappa = 26$ the transition to DO occurs at De_c^∞ and 0.01 Re_c , while at $\kappa = 0.03$ it occurs at 0.14 De_c^∞ and 1.2 Re_c . The properties of DO change with κ [9], but this pattern is hard to study because of its chaotic nature. Therefore, we concentrated on ordered transient NLO (fig. 2) that appear as non-axisymmetric traveling or standing waves with azimuthal wave number $m = 1$ and merge with stable RSW at low κ [9]. (This spatial structure agrees well with recent theoretical predictions [12, 11].) The dependence of the oscillation period, $T_{\text{osc}} = 2\pi/\omega$, and the axial wave number, k , in NLO on κ is shown in fig. 4.

The wave number, k , becomes constant in the limit of large κ . At small κ the wave number is close to 3.15. This is actually the value of k predicted for a purely inertial non-axisymmetric mode in a Newtonian fluid at the same gap ratio, d/R_1 , as in our system [13,9]. This mode has never been observed, though, since its critical Reynolds number is higher than Re_c of axisymmetric TVF. The wave number increase with κ in the crossover region is evidence of changes in the NLO structure there.

At small κ , where inertial effects dominate, T_{osc} is proportional to t_{vd} , and T_{osc}/t_{vd} asymptotically approaches a constant value of about 1, while T_{osc}/λ goes to infinity. In the opposite limit of large κ , where the instability is purely elastic, T_{osc}/λ becomes a constant, while T_{osc}/t_{vd} goes to infinity. The ratio $T_{osc}/T_{rot} \equiv \Omega/\omega$ is constant in both limits. This result is obviously connected to the fact that $t_{vd}\Omega$ and $\lambda\Omega$ become constant in the inertial and the elastic limit, respectively (since $Re \sim t_{vd}\Omega$ and $De \sim \lambda\Omega$). We should note here that for a non-axisymmetric mode, the frequency of oscillations, ω_L , in the reference frame of moving fluid (Lagrangian coordinates) depends on radial position, $\omega_L \cong \omega - m\Omega(R_2 - r)/d$. This frequency also becomes constant at each r in both the inertial and the elastic limits, when measured in units of t_{vd} and λ , respectively. So, the properties of NLO provide a good illustration of the ideas of both hydrodynamic and viscoelastic similarity.

The next step in developing the concept of viscoelastic similarity should be its application to more complex flows. In particular, it was proposed [14] that the efficiency of drag reduction is defined by the Deborah number at the dissipation scale. This suggestion certainly deserves experimental verification. Chaotic spectra of DO [9] show that non-linear elastic effects can lead to spatial-temporal chaos. Therefore, drawing a further analogy between inertial and elastic instabilities, we can suggest that at high enough De elasticity driven turbulence can develop.

This work was partially supported by the Minerva Center For Nonlinear Physics of Complex Systems, by a research grant from the Philip M. Klutznick Fund for Research, and by the Israel Science Foundation grant #92/96-1.

REFERENCES

- [1] BONN D. and MEUNIER J., *Phys. Rev. Lett.*, **79** (1997) 2662; PAKDEL P. and MCKINLEY G. H., *Phys. Rev. Lett.*, **77** (1996) 2459.
- [2] LARSON R. G., SHAQFEH E. S. G. and MULLER S. J., *J. Fluid Mech.*, **218** (1990) 573.
- [3] LARSON R. G., *Rheol. Acta*, **31** (1992) 213.
- [4] SHAQFEH E. S. G., *Annu. Rev. Fluid. Mech.*, **28** (1996) 129.
- [5] BIRD R. B., ARMSTRONG R. C. and HASSAGER O., *Dynamics of Polymeric Liquids*, Vol. 1 (Wiley, New York) 1987.
- [6] DRAIZIN P. G. and REID H., *Hydrodynamic Stability* (Cambridge University press, London) 1981.
- [7] MULLER S. J., LARSON R. G. and SHAQFEH E. S. G., *Rheol. Acta*, **28** (1989) 499.
- [8] BOGER D. V., *J. Non-Newtonian Fluid Mech.*, **3** (1977/78) 87.
- [9] GROISMAN A. and STEINBERG V., *Phys. Rev. Lett.*, **77** (1996) 1480.
- [10] GROISMAN A. and STEINBERG V., *Phys. Rev. Lett.*, **78** (1997) 1460.
- [11] SURESHKUMAR R., BERIS A. N. and AVGOUSTI M., *Proc. R. Soc. London, Ser. A*, **447** (1994) 135.
- [12] JOO Y. L. and SHAQFEH E. S. G., *J. Fluid Mech.*, **262** (1994) 27.
- [13] ROBERTS P. H., *Proc. R. Soc. London, Ser. A*, **283** (1966) 550.
- [14] SURESHKUMAR R., BERIS A. N. and HANDLER R. A., *Phys. Fluids*, **9** (1997) 743.